Molecular Biology of the Cell
Vol. 12, 393–406, February 2001

Prespliceosomal Assembly on Microinjected Precursor mRNA Takes Place in Nuclear Speckles

Ivo Melčák*†‡ Štěpánka Melčáková,*† Vojtěch Kopský,*† Jaromíra Večeřová,*† and Ivan Raška*†§

*Department of Cell Biology, Institute of Experimental Medicine, Academy of Sciences of Czech Republic; †Laboratory of Gene Expression, 1st and 3rd Medical Faculties, Charles University, 128 00 Prague, Czech Republic; and ‡Laboratory of Cell Biology, Howard Hughes Medical Institute, The Rockefeller University, New York, New York 10021-6399

Submitted July 7, 2000; Revised November 3, 2000; Accepted December 19, 2000
Monitoring Editor: Pamela A. Silver

Nuclear speckles (speckles) represent a distinct nuclear compartment within the interchromatin space and are enriched in splicing factors. They have been shown to serve neighboring active genes as a reservoir of these factors. In this study, we show that, in HeLa cells, the (pre)spliceosomal assembly on precursor mRNA (pre-mRNA) is associated with the speckles. For this purpose, we used microinjection of splicing competent and mutant adenovirus pre-mRNAs with differential splicing factor binding, which form different (pre)spliceosomal complexes and followed their sites of accumulation. Splicing competent pre-mRNAs are rapidly targeted into the speckles, but the targeting is temperature-dependent. The polypyrimidine tract sequence is required for targeting, but, in itself, is not sufficient. The downstream flanking sequences are particularly important for the targeting of the mutant pre-mRNAs into the speckles. In supportive experiments, the behavior of the speckles was followed after the microinjection of antisense deoxyoligoribonucleotides complementary to the specific domains of snRNAs. Under these latter conditions prespliceosomal complexes are formed on endogenous pre-mRNAs. We conclude that the (pre)spliceosomal complexes on microinjected pre-mRNA are formed inside the speckles. Their targeting into and accumulation in the speckles is a result of the cumulative loading of splicing factors to the pre-mRNA and the complexes formed give rise to the speckled pattern observed.

INTRODUCTION

Nuclear speckles are enriched in splicing factors and in the factors of the transcription machinery (Spector, 1990; Krause *et al.*, 1994; Bregman *et al.*, 1995; Larsson *et al.*, 1995). Even though there is a consensus that these compartments play a role in RNA metabolism, their exact function is presently unknown. When growing mammalian cells are labeled with antibodies to splicing components, 20 to 50 shining nuclear domains, i.e., nuclear speckles, also termed SC35 domains (protein SC35 being an important serine/arginine (SR)-rich splicing factor [Fu and Maniatis, 1990]), splicing factor compartments, or just speckles, are usually observed (Perraud *et al.*, 1979; Spector *et al.*, 1983; Spector, 1990; Misteli, 2000). In some cell types, they occupy as much as 20% of the nuclear volume. At the electron microscope level, they consist of morphologically well-defined interchromatin granule clusters and of domains of perichromatin fibrils, some of which are believed to represent precursor-mRNAs (pre-mRNAs) (Fakan and Puvion, 1980; Spector *et al.*, 1983; Puvion *et al.*, 1984; Spector, 1990; Fakan, 1994; Raška, 1995; Melčák *et al.*, 2000).

Most mammalian pre-mRNAs contain introns and typically have to be spliced before being transported to the cytoplasm. It has been shown biochemically that spliceosome formation and splicing may be cotranscriptional events (Wuarin and Schibler, 1994). More recent results indicate that transcription and splicing are coupled with interactions of certain factors in both processes. They take part in the large macromolecular complex (termed transcriptosome or mRNA factory), which contains both transcription and splicing factors (Corden and Patturajan, 1997; McCracken *et al.*, 1997; Bentley, 1999).

Splicing components are distributed throughout the nucleoplasm and frequently exhibit local (focal) accumulations.

§ Corresponding author. E-mail: iraska@lf1.cuni.cz.

Abbreviations used: BS-PPT, branch sequence and polypyrimidine tract sequences; oligo, deoxyoligoribonucleotide; DRB, 5,6-dichloro-1-β-D-ribofuranosylbenzimidazole; PPT, polypyrimidine tract; pre-mRNA, precursor messenger RNA; snRNP, small nuclear ribonucleoprotein.

Sites of these accumulations likely represent the sites of active (cotranscriptional) splicing (Neugebauer and Roth, 1997; Misteli and Spector, 1998; Misteli, 2000). However, in growing mammalian cells, many factors of the splicing apparatus are specifically enriched in the speckles (Spector, 1990; Spector *et al.*, 1991; Bregman *et al.*, 1995; Misteli, 2000). At the level of activation of some specific genes, it has been demonstrated that speckles serve as pools of splicing factors that are recruited to the transcription and splicing sites (Huang and Spector, 1996; Misteli *et al.*, 1997).

Primary transcripts of certain genes as well as the spliced RNAs are mapped at sites of active transcription and outside of speckles (Zhang *et al.*, 1994; Smith *et al.*, 1999). On the other hand, pre-mRNAs from some other genes are shown to be associated with nuclear speckles (Xing *et al.*, 1993, 1995; Huang and Spector, 1996; Ishov *et al.*, 1997; Smith *et al.*, 1999; Snaar *et al.*, 1999; Johnson *et al.*, 2000; Melčák *et al.*, 2000). It thus remains unclear as to whether the nuclear speckles reflect localized accumulations of active splicing factors and whether the nucleus is compartmentalized with respect to splicing.

Pre-mRNA splicing consists of two transesterification reactions, which take place in a large ribonucleoprotein complex, the ~60S spliceosomal particle. Spliceosomes are generated by the constitutive assembly of U1, U2, U5, U4/U6 small nuclear ribonucleoprotein particles (snRNPs) and various non-snRNP factors on pre-mRNAs in the cascade of sequence-specific steps (Steitz *et al.*, 1988; Lamm and Lamond, 1993; Moore *et al.*, 1993; Newman, 1994; Krämer, 1996). The formation of the functional spliceosome is thus preceded by the formation of a number of prespliceosomal complexes, termed E, A, and B complexes containing, together with unspliced pre-mRNA, defined combinations of snRNP particles and non-snRNP factors (Steitz *et al.*, 1988; Lamm and Lamond, 1993; Moore *et al.*, 1993; Newman, 1994; Krämer, 1996).

The splicing of pre-mRNAs may be a cotranscriptional event (Beyer and Osheim, 1988; Neugebauer and Roth, 1997; Custodio *et al.*, 1999). However, not all pre-mRNA sequences are processed cotranscriptionally and posttranscriptional splicing does occur (Zachar *et al.*, 1993; Baurén and Wieslander, 1994; Wuarin and Schibler, 1994). Importantly, isolated pre-mRNAs from mammalian cells may contain both introns and poly(A) tails. Splicing may then be a posttranscriptional event, at least in some cases (Alberts *et al.*, 1994; McCracken *et al.*, 1997; Minvielle-Sebastia and Keller, 1999). In this respect, the affinity of microinjected pre-mRNA to speckles has been already demonstrated for the splicing competent exogenous pre-mRNA (Wang *et al.*, 1991; Pederson, 1999). It remains to be established, however, whether these nuclear speckles correspond to the sites of active splicing. On the other hand, it has been demonstrated that microinjected intron-containing RNA is within the cell nucleus processed into functional mRNA (Graessmann and Graessmann, 1982).

The aim of this study has been to expand our knowledge with regard to the function of speckles. We wanted to establish whether the localization of microinjected pre-mRNA with respect to nuclear speckles was the morphological correlate of a certain step in the spliceosomal assembly and whether the individual steps of that assembly were spatially separated. To this end, we microinjected several mutant pre-mRNAs and investigated their accumulation in the speckles. According to biochemical studies (Frendewey and Keller, 1985; Konarska and Sharp, 1986; Bindereif and Green, 1987; Barabino *et al.*, 1990; Hamm and Mattaj, 1990), we inferred that such RNAs permitted the binding of only certain factors and thus mimicked the formation of certain prespliceosomal complexes. By means of a modulation of the distinct steps of spliceosomal formation we assumed to be able to follow the sites of accumulation of (pre)spliceosomal complexes. We also comicroinjected two different mutant pre-mRNAs to follow their respective movement to the speckles. In supportive experiments, we also microinjected antisense oligodeoxyribonucleotides (oligos), complementary to the specific domains of snRNAs. These oligos inhibit splicing throughout the different steps of the spliceosomal assembly (Frendewey *et al.*, 1987; Zillmann *et al.*, 1988; Lamond *et al.*, 1989). This was an alternative approach to generate the "frozen" prespliceosomal complexes on endogenous pre-mRNAs and follow the changes of the speckles. The in vitro formation of at least some splicing complexes is possible with both approaches.

MATERIALS AND METHODS

General Materials

The nucleoside triphosphates (NTPs) were purchased from Sigma Chemical, St. Louis, MO. SP6 and T7 RNA polymerases, RNasin, the nuclear extract, and restriction enzymes were purchased from Promega (Madison, WI). GpppG were purchased from New England Biolabs (Beverly, MA); ChromaTide tetramethylrhodamine-6-UTP (TMR-UTP), ChromaTide Rhodamine Green-5-UTP, lysine fixable fluorescein isothiocyanate (FITC)-dextran from Molecular Probes (Eugene, OR); fluorescein-12-CTP from NEN (Boston, MA); and Cy2-conjugated goat anti-mouse IgG from Jackson ImmunoResearch (West Grove, PA). [α-^{32}P]CTP was purchased from Amersham (Piscataway, NJ) or NEN.

Deoxyoligonucleotides for Pretreatment of Nuclear Extracts

The following oligos were used for the pretreatment of nuclear extracts: U1 (5′-CTCCCCTGCCAGGTAAGTAT-3′), complementary to nucleotides 1–20 of U1 snRNA (Seiwert and Steitz, 1993); U2a (5′-CCAAAAGGCCGAGAAGCGAT-3′), complementary to nucleotides 1–20 of U2 snRNA; and U2b (5′-ATAAGAACAGATACTACACTTGA-3′), complementary to nucleotides 27–49 of U2 snRNA (Lamond *et al.*, 1989). The control oligonucleotide (Ctrl, 5′-TCCGGTACCACGACG-3′) has been described in Pan and Prives (1988) and O'Keefe *et al.* (1994).

Cell Line and Culture

HeLa cells were grown in DMEM (Sigma Chemical), supplemented by 4 mM L-glutamine, 64 μg/ml gentamicin, 0.375% sodium bicarbonate, and 10% fetal bovine serum (Sigma Chemical). The cultures were maintained at 37°C in a 5% CO_2 incubator. The experiments were performed with log-phase growing cultures.

In experiments involving transcription inhibitors, the cells were incubated with 50 μg/ml α-amanitin (Sigma Chemical), 50 μg/ml 5,6-dichloro-1-β-D-ribofuranosylbenzimidazole (Calbiochem, La Jolla, CA) or 4 μg/ml actinomycin D (Sigma Chemical), and grown for 3 h before further use.

Plasmids and Synthesis of RNA Substrates

Plasmids used for the preparation of RNA substrates have been previously described (Frendewey and Keller, 1985). The RNA tran-

scripts were prepared in vitro from a *Sca*I-digested pSP62Δi1 DNA (Ad1, 253 nucleotides), representing the "wild"-type construct from the adenovirus 2 major late pre-mRNA; a *Bst*EII-digested pSP64Δe1Δi1 (Ad2, 78 nucleotides); a *Sca*I-digested pSP64Δe1Δi1.21 (AdM, 187 nucleotides); a *Pvu*II-digested pSP64Δe1Δi1.35 (Ad5, 153 nucleotides); a Fnu D II-digested pSP64Δe1Δi1 (Ad6, 157 nucleotides); a *Sca*I digested pSP64Δe1Δi1 (Ad8, 191 nucleotides); a *Sca*I-digested pSP64Δ5′ (Ad10, 129 nucleotides); a *Bgl*I-digested pSP64Δ5′ (Ad11, 198 nucleotides); and a *Bgl*I-digested pSP64Δe1Δi1 (Ad8^{++}, 260 nucleotides). Plasmids were kindly provided by C. L. Will (University of Marburg, Marburg, Germany; pSP62Δi1) and A. Krämer (University of Geneva, Geneva, Switzerland; pSP64Δe1Δi1, pSP64Δe1Δi1.21, pSP64Δe1Δi1.35, pSP64Δ5′). RNAs containing a branch sequence and a PPT (BS-PPT) were transcribed from DNA templates generated by polymerase chain reaction. DNA template for PIPBS-PPT RNA (34 nucleotides, 5′-GGGUGCUGACUGGCUUCUUCUCUCUUUUUCCCUC-3′ [Query *et al.*, 1997]) derived from pPIP85.B was obtained by polymerase chain reaction from the synthetic oligo (5′-TGCTGACTGGCTTCTTCTCTCTTTTTCCCTC-3′) by using oligonucleotides 77P9 (5′-TAATACGACTCACTATAGGGTGCTGACTGGCTTCTTC-3′), 77R0 (5′-GAGGGAAAAAGAGAGAAG-3′), and DNA for AdBS-PPT RNA (44 nucleotides, 5′-GGGCCUUGAUGAUGUCAUACUUAUCCUGUCCCUUUUUUUUCCAC-3′ [Wansink *et al.*, 1994]) derived from pSP62Δi1 by using oligonucleotides 77R1 (5′-TAATACGACTCACTATAGGGCCTTGATGATGTCATAC-3′), 77R2 (5′-GTGGAAAAAAAAGGGAC-3′).

All pre-mRNAs were transcribed either with SP6 or T7 RNA polymerase. The reaction mixture (25 μl) contained a 1× transcription buffer (Promega), 10 mM dithiothreitol, 1 μg of linearized DNA template, 24 U RNasin, 1 mM GpppG, 50 μM TMR-UTP, 20 U of either SP6 or T7 RNA polymerase in the presence of the nucleotide mixture consisting of 1 mM each of ATP and CTP, 100 μM GTP, and 100 μM UTP. For comicroinjection experiments, green fluorescent RNAs were synthesized with either 50 μM ChromaTide Rhodamine Green-5-UTP in the transcription reaction described above or 50 μM fluorescein-12-CTP in modified nucleotide mixture of 1 mM each of ATP and UTP, 100 μM CTP, and 100 μM GTP. Synthesis of the ^{32}P-labeled RNA was carried out in 25 μl of reaction containing a 1× transcription buffer (Promega); 10 mM dithiothreitol; 0.5 mM each of ATP, UTP; 50 μM GTP; 12 μM CTP; 30 μCi [α-^{32}P]CTP (800 Ci/mmol); 0.5 mM GpppG; 20 U of SP6 RNA polymerase; 24 U of Rnasin; and 1 μg of linearized DNA template. After a 1-h incubation of the reactions at 37°C, an additional 20 U of RNA polymerase were added and incubated for another 1 h. A parallel transcription reaction was carried out with [α-^{32}P]CTP but with 2:1 M ratio of UTP and TMR-UTP (100 and 50 μM, respectively).

The DNA templates were digested with 12.5 U of RQ1 RNase-Free Dnase (Promega) for 15 min at 37°C. The RNA transcripts were then purified by means of electrophoresis on either 6 or 8% polyacrylamide gels containing 7 M urea followed by the excision and elution of the RNA from the gel pieces in 0.75 M ammonium acetate, 10 mM magnesium acetate, 0.1% (wt/vol) SDS, 0.1 mM EDTA overnight at 37°C. The eluted RNA was separated from the gel pieces by a Millipore Ultrafree-MC filter unit (0.45 μm), ethanol precipitated and dissolved in nuclease-free water at a concentration of ~50 μg/ml, and stored at −70°C.

In Vitro Splicing Assay and Pretreatment of Nuclear Extracts with Deoxyoligoribonucleotides

Splicing reactions (6.25 μl) containing uniformly labeled pre-mRNA (2×10^3 cpm) were performed at 30°C in a solution of 32% HelaSplice nuclear extract (Promega), 1× splicing buffer extract (Promega), 3 mM $MgCl_2$, and 1 unit RNasin. After incubation, which lasted 15 min, the splicing reactions were loaded directly onto a 4% polyacrylamide, 50 mM Tris-glycine gel (acrylamide to bisacrylamide, 80:1; Konarska and Sharp, 1987) and the complexes were visualized by autoradiography.

The pretreatment of the nuclear extracts with antisense deoxyoligonucleotides was performed by incubating with 26 μM each of U1, U2a, U2b, Ctrl oligonucleotides in a separate tube for 10 min at 30°C before adding the splicing substrate.

The splicing competency of fluorochrome-labeled RNA (1×10^5 cpm) was tested in splicing reactions (25 μl) as described above for the indicated times, followed by phenol extraction, ethanol precipitation, electrophoresis in an 12% polyacrylamide/8.3 M urea gel, and autoradiography.

Microinjection and Immunolabeling

For the routine RNA microinjection experiment, 1 μl of RNA was mixed with 0.4 μl of 17.5 mM Tris-acetate pH 6.95. To avoid capillary clogging, the solution was clarified through centrifugation at 19,000 × *g* (Hettich, Tuttlingen, Germany) for 15 min. The microinjection solution was loaded into microinjection needles (Femtotips; Eppendorf, Hamburg, Germany) and microinjection was performed by using IX70 inverted microscope (Olympus Optical, Tokyo, Japan) connected to Micromanipulator 5170 and Microinjector 5242 (Eppendorf, Hamburg, Germany). The nuclei of HeLa cells grown at lower density on CELLocate microgrid coverslip (Eppendorf) were microinjected within 5 to 10 min after their removal from the 37°C culture incubator. In each experiment, 20–60 cells were microinjected. Not all microinjected cells could be subsequently investigated because, for example, a few microinjected cells detached from the support or disrupted. The cells were then washed with a fresh prewarmed medium and incubated at 37°C for 30 min (unless specified otherwise; 30-min incubation period was used in the comicroinjection experiments) before fixation. The oligos were injected into the cytoplasm of the cells according to O'Keefe *et al.* (1994). To monitor the proper cytoplasmic microinjection, the oligonucleotides were injected with 1–3 mg/ml lysine fixable FITC-dextran (mol. wt. 70.000). After microinjection, the cells were washed and incubated at 37°C for 30 min. The detection of the splicing factor SC35 was performed according O'Keefe *et al.* (1994) with slight modifications. The cells were washed and fixed for 10 min with 2% formaldehyde in phosphate-buffered saline (PBS) and permeabilized with 0.2% Triton X-100 in PBS for 5 min at room temperature. The cells were washed and then incubated with an anti-SC35 antibody (Fu and Maniatis, 1990; kindly provided by X.-D. Fu, University of California, San Diego, CA) for 30 min. The cells were washed and then incubated with Cy2-conjugated goat anti-mouse secondary antibody for 30 min. The cells were washed and dried. The detection of transcription signal in microinjected cells due to the incorporated bromouridine was performed as described in Koberna *et al.* (1999). All washes were conducted with PBS, pH 7.4. The coverslips were mounted on glass slides in 2.3% (wt/vol) Mowiol 40-88 (Sigma Chemical)/42.5% glycerol/0.1 M Tris-HCl pH 8.5 containing 134 mM 1,4-diazabicyclo[2.2.2]octane to reduce fading.

Digital Imaging Microscopy

The samples were examined by using an epifluorescence microscope AX70 Provis (Olympus Optical) fitted with a cooled charge-coupled device camera PXL (Photometrics, Tucson, TX) with KAF-1400 chip. A universal planfluorit 60/1.25 N.A. objective was used. The images were captured by using IPLab Spectrum (Signal Analytics, Vienna, VA) software. To achieve dual color labeling, a combination of either single band excitation and emission filters (Rhodamine Green, tetramethylrhodamine) or single band blue (Cy2, FITC), green (tetramethylrhodamine) exciters and triple bandpass emission filter (Chroma Technology, Brattleboro, VT) were used. The images were corrected for dark field current and background. The contrast and opacity were optimized for each channel. The colocalization was performed by merging the individual channels with IPLab Spectrum (Signal Analytics). The images were printed on a Phaser 440 Color Printer (Tektronix, Wilsonville, OR) by using Adobe Photoshop (Adobe Systems, Mountain View, CA).

RESULTS

In the experiments described below, we identified the speckles with the SC35 domains by means of imunocytochemistry with anti-SC35 antibodies. We assumed that the microinjected wild-type and mutant pre-mRNAs did bind with relevant nuclear factors as inferred from previous biochemical findings in vitro. Keeping in mind the composition of this macromolecular complex, we investigated its localization with regard to the nuclear speckles.

It should be emphasized that the microinjection of several tens of cells always took a few minutes at room temperature. Therefore, some movement of pre-mRNAs could take place during the course of the microinjection procedure. However, we kept this phenomenon under some control because we knew the order of microinjected cells on the CELLocate coverslips.

Movement of Splicing Competent Pre-mRNA to Speckles Is Rapid

Wang *et al.* (1991) demonstrated pre-mRNA trafficking to nuclear speckles of several intron-containing RNAs (β-globin, proenkephalin, or adenovirus origin) after microinjection. We confirmed these findings with intron-containing, fluorochrome-labeled, and splicing-competent RNAs derived from adenovirus 2 major late construct (Frendewey and Keller, 1985), which were microinjected into the nuclei of living HeLa cells. As shown in Figure 1, the fluorochrome-labeled RNA was spliced to approximately the same extent as unlabeled RNA. Immediately after microinjection, the RNA was distributed throughout the nucleoplasm (our unpublished results). Over the next 5–60 min, the RNA localized to speckles (Figure 2, A and B). During longer periods, the RNA was still concentrated in the speckles, but the intensity of fluorescence decreased (our unpublished results).

In addition, we investigated whether the exogenous microinjected pre-mRNA is also accumulated in speckles in transcriptionally silent cells. In a parallel experiment, HeLa cells were incubated with 50 μg/ml α-amanitin, 50 μg/ml 5,6-dichloro-1-β-D-ribofuranosylbenzimidazole, or 4 μg/ml actinomycin D for 3 h and then microinjected with pre-mRNA. Movement to enlarged/rounded up SC35 domains, which is typical for transcriptionally inhibited cells (Sinclair and Brasch, 1978; Spector *et al.*, 1991; Melčák *et al.*, 2000), was not abolished (our unpublished results). This indicated that the movement of microinjected RNAs to the speckles was independent of the ongoing nuclear transcription.

Movement of Splicing Competent Pre-mRNA into Speckles Is Temperature-dependent

A 5-min incubation period at 37°C of microinjected cells resulted in the rapid trafficking of pre-mRNA to speckles (Figure 2A). Most of the fluorescent label was still nucleoplasmic, but the higher intensity inside and around the speckles was clearly noted (Figure 2A, arrowheads). Much of the fluorescence signal was found inside the speckles after 15 min of incubation (Figure 2B), but some pre-mRNA signal adjacent to the speckles (Figure 2B, arrowheads) was still detected. The very rapid kinetics of pre-mRNA trafficking to the speckles could be inferred, pointing also to the importance of the vicinal space surrounding the speckles.

A striking difference in pre-mRNA trafficking was noted when the microinjected cells were kept at 4°C for 30 min (Figure 2C). The morphology of the speckles changed (Figure 2C). Much of the fluorescence label was found adjacent to the speckles, usually in the form of distinct dots. These results indicate that the movement of pre-mRNA within the interchromatin space toward the speckles was possibly a diffusion process (Politz *et al.*, 1999), but the targeting inside the speckles themselves was temperature-dependent. The results of the experiments in which we microinjected the Ad1 RNA labeled with red fluorochrome and after 15 min of incubation at 37°C microinjected the same cells with the Ad1 RNA labeled with green fluorochrome and incubated for 30 min at 4°C supported this view (Figure 2D). Apart from the overall nuclear green fluorescence, the RNA labeled with green fluorochrome accumulated also adjacent to the red "speckles" generated by the accumulation of RNA labeled with red fluorochrome (Figure 2D, arrowheads). The red label remained associated with the speckles, pointing to the irreversibility of the targeting process.

In this set of experiments, we have shown that the movement of pre-mRNA toward the speckles corresponded apparently to diffusion. In contrast, the massive accumulation of RNAs within the speckles was temperature-dependent, and was irreversible.

Pre-mRNA Structural Requirements for its Targeting to the Speckles

We subsequently investigated the movement of various mutant (altered or truncated) pre-mRNA to speckles, and also examined the effects of the second exon and intron, which are known for their role in the prespliceosome assembly (Hoffman and Grabowski, 1992; Staknis and Reed, 1994). Biochemical studies have suggested that the formation of the prespliceosome complex was blocked and that the kinetics of the splicing process were thus influenced at different stages of the splicing reaction.

The described particular fluorescence pattern (see below) was observed in 79–94% of microinjected cells for the various RNAs. Importantly, the described pattern was observed in at least 89% of microinjected cells with those RNAs (i.e., Ad8, Ad8^{++}, Ad10, and Ad11 RNAs), which heavily accumulated in the speckles identified through the SC35 immunolabeling.

The Ad2 RNA (Figure 3A) is incapable of forming detectable (pre)splicing complexes resolved in native gels (Frendewey and Keller, 1985; Hamm and Mattaj, 1990). However, such mutant RNA (with deleted or altered branch sequence/3′ splice site region) is able to bind U1 snRNP (Bindereif and Green, 1987; Vankan *et al.*, 1992; Rossi *et al.*, 1996) and form the complex analogous to E complex, designated as E5′ (Michaud and Reed, 1993; Staknis and Reed, 1994). When this RNA was microinjected, it was targeted toward the speckles and formed tiny dots adjacent to the speckle. We did not notice any differences between the fluorescence pattern of Ad2 and AdM RNAs (our unpublished results). The AdM RNA is similar to the Ad8 RNA (see below) except for the mutated polypyrimidine tract (PPT) sequence.

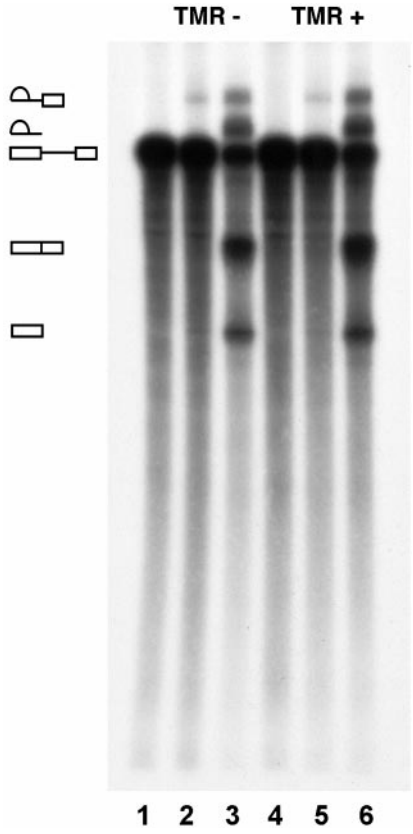

Figure 1. In vitro splicing of tetramethylrhodamine-labeled Ad1RNA. Lanes 1–3, unlabeled (TMR−) Ad1 RNA; lanes 4–6, tetramethylrhodamine-labeled (TMR+) Ad1 RNA. The splicing reactions were performed for 0 (lanes 1 and 4), 30 (lanes 2 and 5), and 90 min (lanes 3 and 6). The positions of splicing intermediates and products are indicated at the left of lane 1.

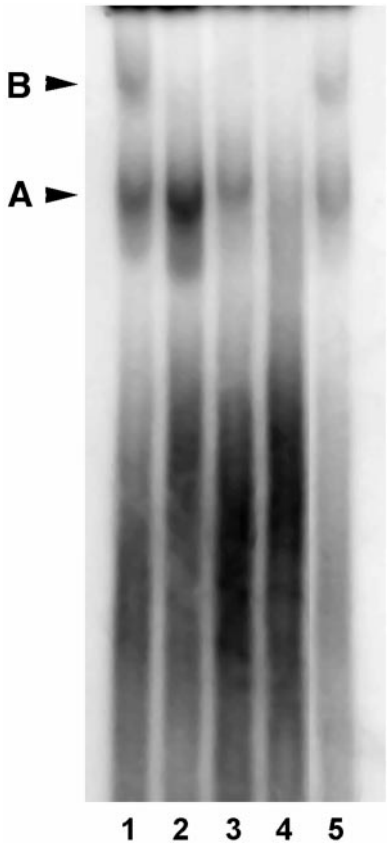

Figure 5. Native gel documenting the role of antisense oligos in the formation of spliceosomal complexes A and B (indicated by arrows). Lane 1, no oligo added; lane 2, U1 oligo; lane 3, U2A oligo; lane 4, U2b oligo; lane 5, control oligo. See text for the detailed description.

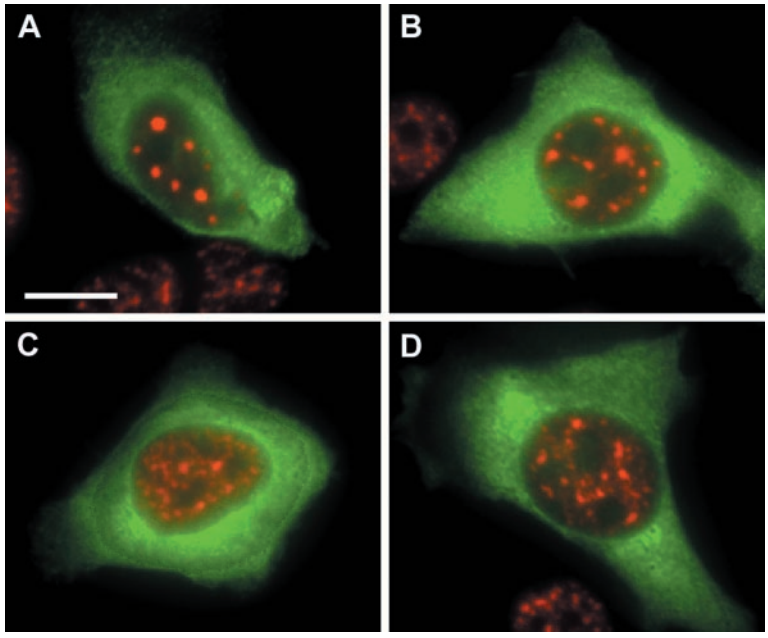

Figure 6. HeLa cells microinjected with antisense oligos and dextran-fluorescein were after incubation labeled for the SC35 protein (in red). U1 oligo (A), U2a oligo (B), U2B oligo (C), unrelated oligo (D); the appearance of the speckles in untreated cells (part of the nuclear profile is seen) is the same. See text for the detailed description.

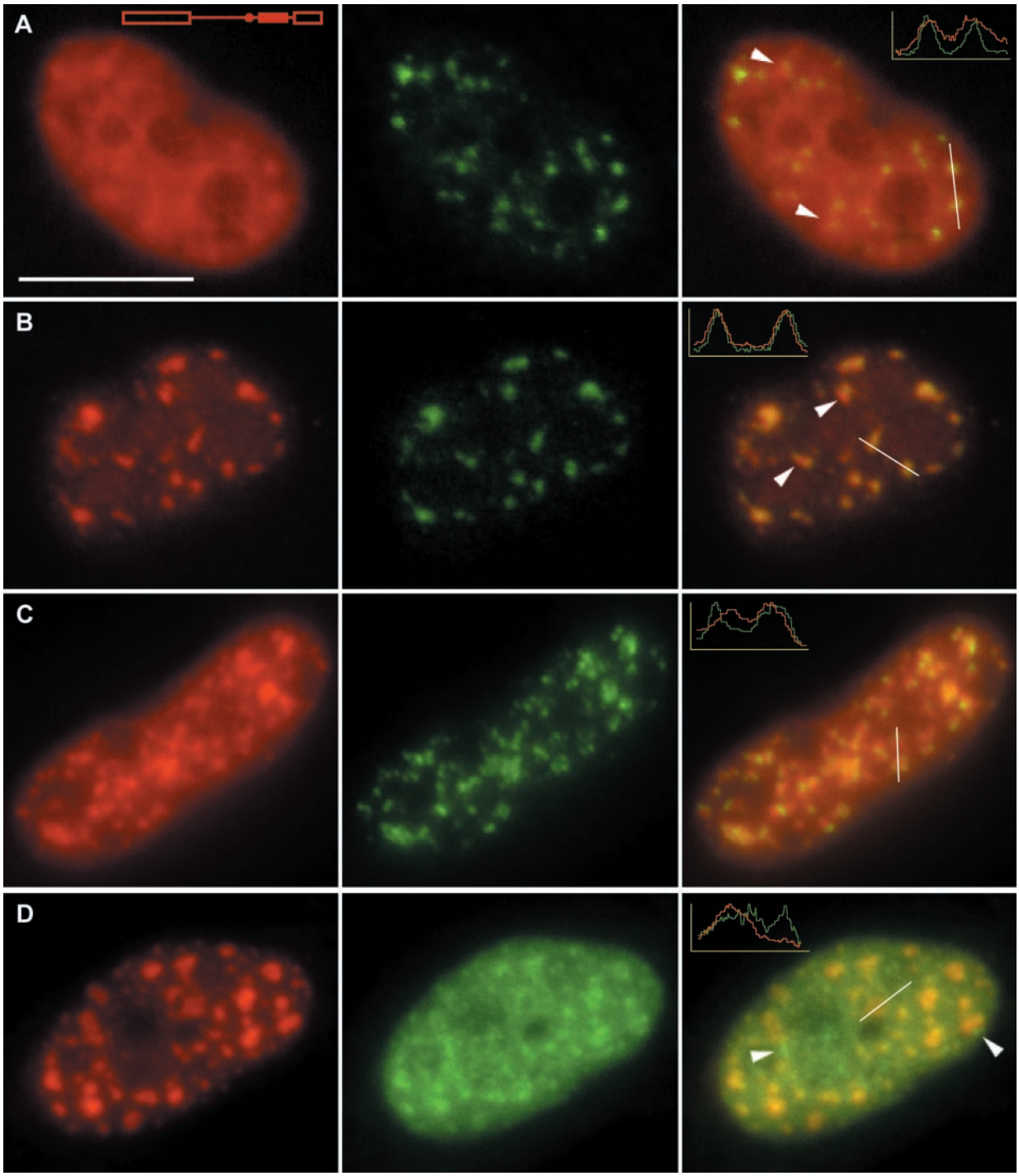

Figure 2. HeLa cells observed after microinjection of the fluorochrome-labeled Ad1 RNAs. The two left columns correspond to individual color channels, the right column is the overlay. The structure of the Ad1 RNA is shown. The cells were labeled for SC35 protein (in green) after 5-min (A) or 15-min (B) incubation at 37°C, or after 30-min incubation at 4°C (C). Note that the Ad1 RNA (in red) accumulates in the vicinity of speckles in A (arrowheads), such an accumulation is still occasionally seen in B (arrowheads). A striking accumulation of the Ad1 RNA adjacent to the speckles is seen in C. (D) After the consecutive microinjection of the Ad1 RNA labeled with red fluorochrome (the cells being shortly incubated at 37°C) and of the Ad1 RNA labeled with green fluorochrome, the cells were incubated at 4°C for 30 min. Note the differences in red and green fluorescence patterns, the red signal being engulfed within the green signal (arrowheads). For the quantitative evaluation (inserts in Figures 2 and 3, A–E), fluorescent intensities along the segments shown in Figures 2 and 3, A—E, were scaled to the minimum and maximum values. The identical position of peaks in the two color channels testifies to the accumulation of RNAs in the speckles. The bar in Figures 2–4 and in Figure 6 designates 10 μm.

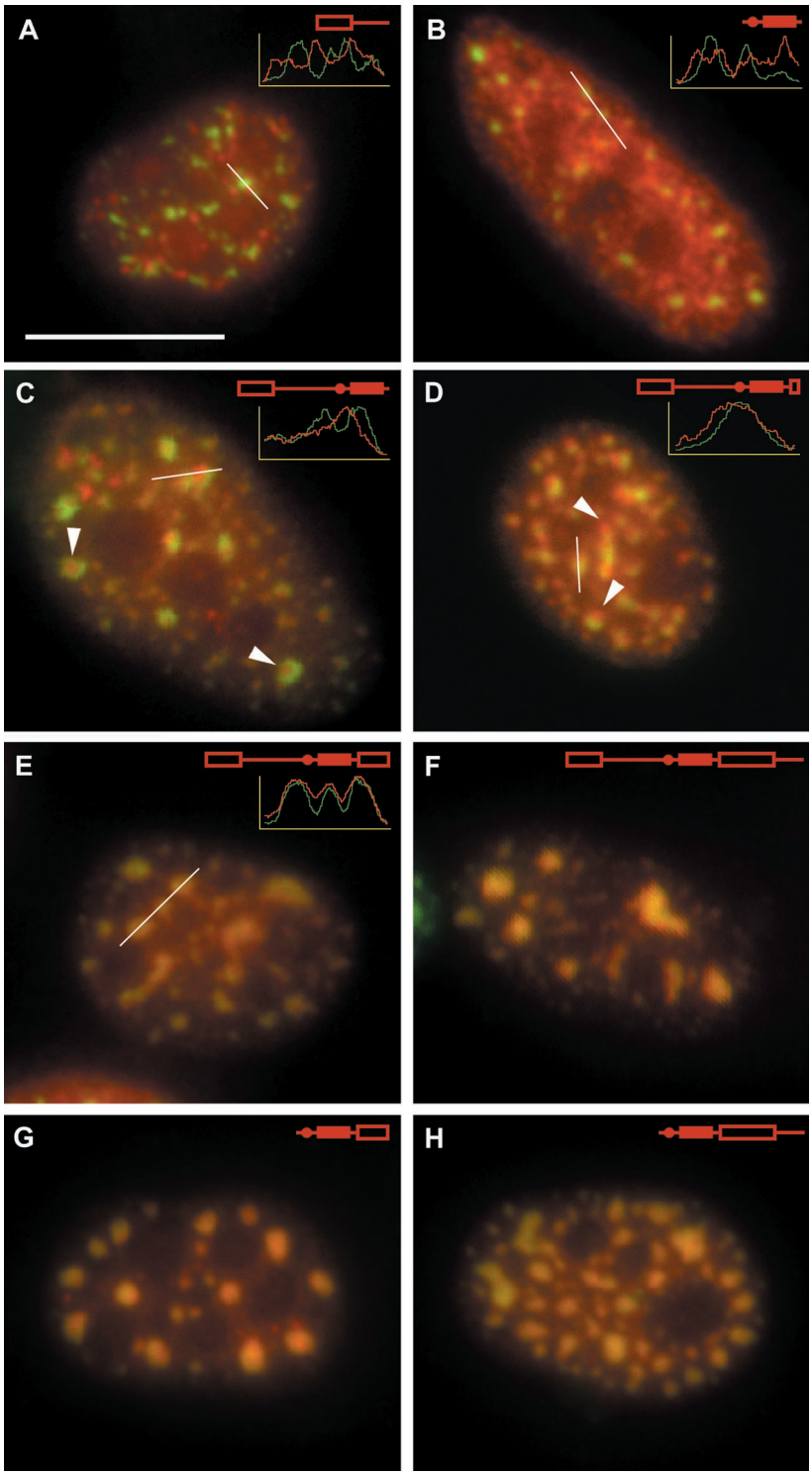

Figure 3. The HeLa cells microinjected with various mutant pre-mRNAs (labeled with red fluorochrome) documenting the structural requirements for their targeting to the speckles. After the incubation, the cells were labeled for SC35 protein (in green). The structure of microinjected RNAs is shown. Ad2 RNA (A), AdBS-PPT RNA (B), Ad5 RNA (C), Ad6 RNA (D), Ad8 RNA (E), Ad8^{++} RNA (F), Ad10 RNA (G), and Ad11 RNA (H). See text for the detailed description.

The AdBS-PPT RNA (Figure 3B) and PIPBS-PPT RNA (our unpublished results), which both consist of just BS and PPT, generated a fluorescence pattern with RNAs staying outside of the speckles. These RNAs form merely a minimal splicing complex Amin (Query *et al.*, 1997). The RNAs also displayed some tendency to be targeted toward the speckles and their accumulations were often found adjacent to the speckles in the form of distinct dots or streaks.

With the Ad5 RNA (Figure 3C), the first step of splicing may proceed and enables a formation of lariat. The kinetics

are, however, very weak (Frendewey and Keller, 1985). Following microinjection, the mutant pre-mRNA stayed outside of the speckles, but its frequent association with the speckles was well apparent. Sometimes, the generated pattern of the speckles was in the form of "doughnuts," exhibiting domains deficient in splicing factors (Figure 3C, arrowheads).

The Ad6 RNA is similar to the Ad5 RNA, but also contains four nucleotides of the second exon (Figure 3D). It forms the splicing complex more efficiently, but the short second exon is not sufficient for complete splicing (Frendewey and Keller, 1985). In contrast to the previous three fluorescence patterns, the accumulation of microinjected mutant pre-mRNA within the somewhat enlarged speckles was already well apparent, with fluorescent dots still being associated with the periphery of speckles (Figure 3D, arrowheads).

The splicing competent construct Ad8 (Figure 3E) is almost identical to the Ad1 RNA, but has partial deletion in the leader 1 exon. Microinjected mutant pre-mRNA was found within the speckles, which were larger than those with the Ad1 RNA, reflecting possibly the slower kinetics of the 35S prespliceosomal complex A as described by Frendewey and Keller (1985).

The splicing competent Ad8^{++} RNA contains in addition the complete exon 2 and the first 35 nucleotides of the intron 2, the 5′ downstream splice site enhancing the utilization of the upstream 3′ splicing site (Freyer *et al.*, 1989), probably through the U1 snRNP binding (Hwang and Cohen, 1996; Yue and Akusjärvi, 1999). Microinjected mutant pre-mRNA was found within the enlarged speckles (Figure 3F).

The Ad10 RNA, with the first exon and part of the 5′ intron sequence deleted with respect to the Ad8 RNA, enables only the assembly of the presplicing complex A, denoted as complex A3′ (Frendewey and Keller, 1985; Christofori *et al.*, 1987; Frendewey *et al.*, 1987). The microinjected mutant pre-mRNA was accumulated in the enlarged speckles (Figure 3G).

In contrast to the Ad10 RNA, the longer runoff transcripts of Ad11 RNA contained a complete exon 2 and also a part of the second intron, which resulted in an RNA that has 5′ and 3′ splice sites, but not in the usual orientation. Similarly to the Ad10 RNA, this RNA is able to form prespliceosomal complex A3′, but not the functional spliceosome (Frendewey and Keller, 1985). The microinjected Ad11 RNA was also accumulated in the enlarged speckles (Figure 3H). The results of the two last experiments underlined the importance of the PPT sequences and the downstream sequences for the movement of RNAs into the speckles and indicated that presplicing complexes formed on the relevant nonspliceable mutant pre-mRNAs were accumulated in the speckles.

In the last four experiments with the microinjected Ad8, Ad8^{++}, Ad10, and Ad11 RNAs (Figure 3, E–H), a notable increase in the size of the speckles was observed reflecting the accumulation of splicing factors, together with mutant pre-mRNAs. In addition, the increase in size was sometimes accompanied by the rounding up of the speckles. Importantly, after the microinjection of mutant RNA (such as the Ad10 RNA), we detected RNA transcription signal due to incorporated bromouridine outside of the speckles (our unpublished results). The microinjection apparently did not interfere with the nuclear transcription because the RNA synthesis pattern was similar to that seen in nonmicroinjected cells (our unpublished results). So, we assume that microinjected cells behave within the physiological range.

This series of experiments showed that the movement to, and the accumulation in, the speckles of mutant pre-mRNA depended on its sequence and was strictly correlated with the ability to form the (pre)spliceosomal complexes. The 3′ end of the first intron, including the PPT, however, was necessary but insufficient for the targeting into the speckles. It was particularly dependent on the flanking downstream sequences. The targeting of such RNAs into the speckles resulted in an increase in the size, and frequently in a rounding up, of the speckles.

Different Mutant Pre-mRNAs Exhibit Different Targeting and Compete for the Accumulation in the Speckles

In the next series of experiments, we comicroinjected two mutant pre-mRNAs labeled with different fluorochromes to establish their respective accumulation in the speckles. First, we performed comicroinjections of two identical RNAs labeled, however, with different fluorochromes (see the microinjected Ad6 in Figure 4A). The fluorescence pattern was the same for the two RNAs as documented by the uniform yellow color. This demonstrated that the different types of fluorochromes used did not alter the movement of the mutant pre-mRNAs.

The comicroinjection of the Ad2 and AdM RNAs resulted in an almost identical localization of the two mutant pre-mRNAs in many tiny fluorescent dots (Figure 4B) located adjacent to the speckles (cf. Figure 3A). The comicroinjection of the Ad2 (red) and Ad10 (green) RNAs resulted in differential targeting. The Ad10 RNA accumulated in the speckles, whereas the Ad2 RNA accumulated adjacent to the speckles (Figure 4C).

After the comicroinjection of the Ad5 (red) and Ad6 (green) RNAs, the Ad6 was seen in the speckles and also in domains adjacent to the speckles (Figure 4D). These domains were also enriched with Ad5 RNA (Figure 4D, arrowheads). A similar result was observed when the Ad6 (red) and Ad8 (green) RNAs were comicroinjected (Figure 4E), with the Ad8 RNA showing greater accumulation in the speckles. A striking difference in the fluorescence pattern was observed after comicroinjection of the Ad5 (green) and Ad8 (red) RNAs. The speckles were larger and the Ad8 RNA accumulated in the speckles. The Ad5 RNA, in accordance with the results of individual miroinjections (Figure 3C), was seen in distinct dots usually at the periphery of the speckles and/or in the Ad8 RNA deficient areas within the speckles (Figure 4F, arrowheads).

When the Ad8 (red) and Ad10 (green) RNAs were comicroinjected, both RNAs accumulated in the speckles (Figure 4G). A similar result was observed when the Ad8^{++} (red) and Ad11 (green) RNAs were comicroinjected (Figure 4H).

The fluorescence patterns of the above series of experiments were in agreement with the results of individual microinjections (see Figure 3). In contrast, qualitative differences were observed in the next three experiments.

The following two results reflected the importance of the second exon and/or downstream 5′ splice site in the targeting into the speckles. Although both Ad8 and Ad8^{++} RNAs,

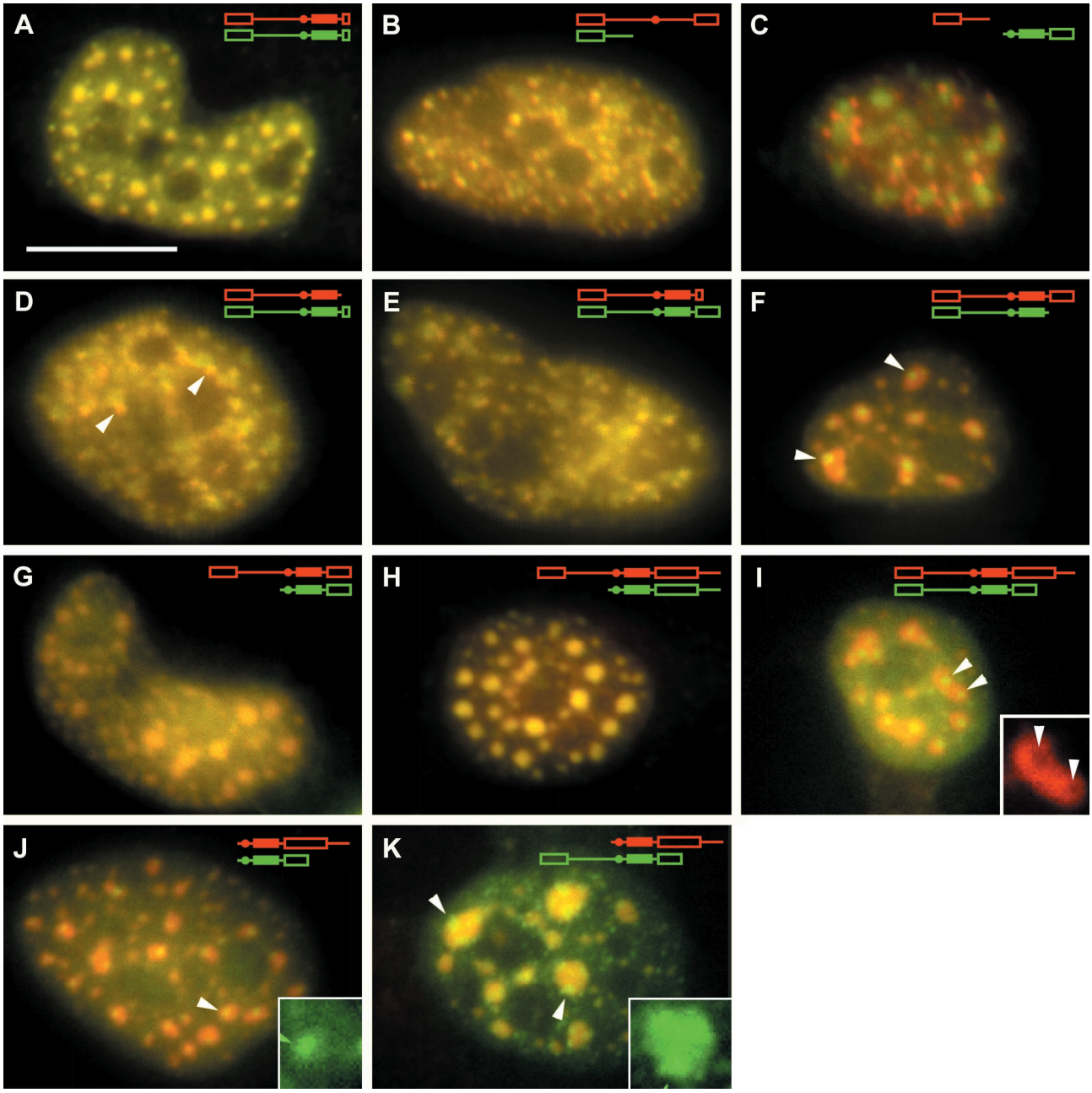

Figure 4. HeLa cells comicroinjected with two mutant pre-mRNA labeled with two different fluorochromes. The structure of comicroinjected RNAs is shown. Ad6 and Ad6 RNAs (A), Ad2 and AdM RNAs (B), Ad2 and Ad10 RNAs (C), Ad5 and Ad6 RNAs (D), Ad6 and Ad8 RNAs (E), Ad5 and Ad8 RNAs (F), Ad8 and Ad10 RNAs (G), Ad8^{++} and Ad11 RNAs (H), Ad8 and Ad8^{++} RNAs (I) (one color channel insert shows the Ad8 $^{++}$RNA deficient areas [see arrowheads in I]), Ad10 and Ad11 RNAs (J) (detail in one channel insert depicts the Ad10 RNA displacement from the speckle), and Ad8 and Ad11 RNAs (K) (detail in one channel insert shows the presence of the Ad8 RNA within the speckle). See text for the detailed description.

which are able to form the functional spliceosome, were efficiently targeted to speckles when microinjected individually, the comicroinjection of the Ad8 (green) and Ad8^{++} (red) RNAs resulted in a different pattern (Figure 4I). Although a prominent accumulation of the Ad8^{++} RNA in the speckles was seen as in the case of the individual microinjections, the Ad8 RNA generated fluorescence dots associated with and/or embedded in the speckles. These dots were usually seen in Ad8^{++} RNA-deficient areas (Figure 4I, arrowheads; see also the red channel detail in the insert). A somewhat similar result was observed if Ad10 (green) and Ad11 (red) pre-mRNA mutants were comicroinjected (Fig-

ure 4J). Both RNAs were unable to form the functional spliceosome, but the prespliceosomal complex A3′ (Frendewey and Keller, 1985; Christofori *et al.*, 1987) and the individual microinjections resulted in their accumulation in the speckles (Figure 3, G and H). Here, however, the speckles were reddish with yellowish dots in the periphery of and/or embedded in the speckles (Figure 4J, arrowhead; see the detail of one speckle [green channel] in the insert) pointing to a displacement of the Ad10 RNA compared with the individual microinjections (Figure 3G).

With regard to the last two experiments, the Ad8 (green) and Ad11 (red) RNAs enable the formation of different complexes, functional spliceosome and prespliceosomal complex A3′, respectively (Frendewey and Keller, 1985). Even though the comicroinjected Ad8 RNAs were not displaced from the speckles as efficiently as was the displacement in the two previous experiments, it was still enriched in green dots in the periphery of and/or embedded in the speckles (Figure 4K, arrowheads; see the detail of one speckle [green channel] in the insert). Despite the fact that this comicroinjection experiment involved RNAs capable of forming different (pre)spliceosomal complexes, this finding pointed to the importance of the second exon and/or the downstream 5′ splice site in the efficient targeting to the speckles.

The results of this set of experiments supported the findings established with the microinjections of the individual mutant pre-mRNAs. In addition, however, depending on the sequence of the microinjected RNAs, the RNAs competed for their accumulation within the speckles.

Appearance of Speckles Is Changed after Microinjection of Antisense Deoxyoligoribonucleotides That Block Assembly of Prespliceosomal Complex Formation during a Specific Step of the Splicing Reaction

In the experiments described above, we observed a correlation between the targeting of RNAs into the speckles and the subsequent increase in their size. Results with the microinjected RNAs showing changes in the size of the speckles were corroborated by analogous experiments in which antisense oligos were used to block the assembly of specific prespliceosomal complexes on endogeneous RNAs.

We used three different oligos, anti-U1 snRNA and anti-U2a oligo with an affinity to 5′ end of U1 and U2 snRNA, respectively (Lamond *et al.*, 1989; Seiwert and Steitz, 1993), and anti-U2b oligo with an affinity for the central sequence of U2 snRNA (Lamond *et al.*, 1989). First, we documented the spliceosome complex formation in the nuclear extracts treated with oligos that inhibit splicing in vitro (Figure 5). Antisense oligo to U1 snRNA (nucleotides 1–20) induced a block of the formation of the prespliceosomal complex B, but had no effect on the generation of the presplicing complex A (Figure 5B). This indicated that the 5′ proximal region of U1 snRNA was necessary for the spliceosome formation, but it was not required for the generation of the presplicing complex A (Frendewey *et al.*, 1987; Hamm *et al.*, 1989; Barabino *et al.*, 1990). A similar effect was observed with oligo U2a against the 5′ segment of U2 snRNA (nucleotides 1–20). This oligo did not block completely the formation of the prespliceosome complex A (Lamond *et al.*, 1989), but the formation was already reduced (Figure 5C). A different effect was observed with oligo U2b against the internal segment of U2 snRNA (nucleotides 27–49). Under these conditions, the presplicing complex formation was completely blocked (Figure 5D; Hamm *et al.*, 1989; Lamond *et al.*, 1989).

At the cell level, we performed the microinjection of oligos, together with fluorescein-labeled dextran, into the cytoplasm of HeLa cells. After a 30-min incubation at 37°C we performed the labeling of SC35 domains (in red, Figure 6).

The microinjection of the anti-U1 oligo into the cytoplasm led to the formation of large and rounded up speckles (Figure 6A). Somewhat enlarged, but not so round, speckles were formed after the microinjection of the anti-U2a oligo (Figure 6B). The microinjection of the anti-U2b oligo (Figure 6C), which blocked the prespliceosomal complex formation completely, did not alter the appearance of the speckles, the pattern of which was compatible with that seen in cells microinjected with the unrelated oligo (Figure 6D). Importantly, the changes in the speckle pattern are fully reversible. The signal in the form of rounded and enlarged speckles peaked after ~30 to 45 min, and then the signal changed and normal speckles, identified through the SC35 signal, reappeared after ~2 h.

These results complemented those obtained with microinjected RNAs and indicated that the enlargement of the speckles, due to the accumulation of splicing factors, apparently reflected the accumulation of "frozen" presplicing complexes formed in the speckles on endogenous pre-mRNAs.

DISCUSSION

Many aspects of the biochemistry of the splicing process are known in great detail (reviewed in Mattaj, 1994; Sharp, 1994; Manley and Tacke, 1996; Newman, 1998; Lamond, 1999). However, we know little about the function of speckles. The only established function of this compartment is that it serves as a reservoir of splicing factors (Huang and Spector, 1996; Misteli *et al.*, 1997). To expand our knowledge of the function of speckles, we used the microinjection approach, which allowed us to study the RNA targeting and the accumulation kinetics.

In agreement with the findings of Wang *et al.* (1991), the results of this study show the movement of microinjected precursor pre-mRNA to the nuclear speckles in HeLa cells. After 15 min of incubation, much of this pre-mRNA was found inside the speckles. This RNA movement persists in transcriptionally inhibited cells. The movement of endogenous pre-mRNA to the speckles has been demonstrated in both transcriptionally active and silenced cells (Xing *et al.*, 1995; Dirks *et al.*, 1997; Ishov *et al.*, 1997; Smith *et al.*, 1999; Snaar *et al.*, 1999; Johnson *et al.*, 2000; Melčák *et al.*, 2000). In addition, it has been shown that microinjected intron-containing RNA is within the cell nucleus processed into functional mRNA (Graessmann and Graessmann, 1982) and that several microinjected RNAs transcribed by RNA polymerase II and III localized at specific nuclear sites at which their corresponding endogenous counterparts were present in the steady-state distribution as shown by in situ hybridization (Jacobson *et al.*, 1995, 1997; Jacobson and Pederson, 1998a,b; Pederson, 1999). These findings support the concept that microinjected pre-mRNAs behave in a manner similar to endogenous pre-mRNAs.

The targeting of pre-mRNA to speckles is impeded at 4°C. These findings point to the possible existence of the energy-dependent step, which is irreversible. Because microinjected RNAs accumulate around the speckles even at 4°C, we infer that the movement of RNAs consists of two steps: the movement of pre-mRNAs toward the speckles is probably the diffusion process (Politz *et al.*, 1999) and their targeting within the speckles is likely an energy-dependent process.

The results with mutant pre-mRNAs indicate that the (pre)spliceosomal assembly takes place inside the nuclear speckles. Targeting to, and accumulation within, the speckles depends on the nucleotide sequence of the microinjected RNAs. It has been demonstrated (Wang *et al.*, 1991) that microinjected intronless RNAs or RNAs with deleted PPT and 3′ splice site are not targeted to the speckles. We expanded these results with mutant pre-mRNAs, which, according to biochemical studies, generate splicing complexes during various steps of the splicing reaction (Frendewey and Keller, 1985). We observed the correlation between the prespliceosomal complex formation established in in vitro experiments and targeting of microinjected RNAs to speckles. Accordingly, we show that PPT is necessary, but is not in itself sufficient for the targeting of RNAs into the speckles. Particularly important for the targeting to the speckles are the flanking downstream sequences to the 3′ splice site. We emphasize that the targeting also takes place in the case of nonspliceable RNAs Ad10 and Ad11, which are able to form prespliceosome complexes in vitro (Frendewey and Keller, 1985; Christofori *et al.*, 1987; Frendewey *et al.*, 1987).

It has been established that the E (early) complex formation (Seraphin and Rosbash, 1989; Bennett *et al.*, 1992; Michaud and Reed, 1993) as well as complexes formed on the minimal RNA substrate consisting of BS and PPT sequence (called Amin complex) (Query *et al.*, 1997) do not in vitro require ATP (Legrain *et al.*, 1988; Michaud and Reed, 1991; Jamison *et al.*, 1992; Query *et al.*, 1997). The first ATP-dependent step involves the formation of an A complex, respectively A3′ complex (Konarska and Sharp, 1986; Query *et al.*, 1997). In this respect, the results with mutant pre-mRNAs correlate well with those performed at 4°C. The Ad2, AdM, and BS-PPT RNAs display a tendency to be targeted toward the speckles and remain accumulated around or in the proximity of the speckles in the form of distinct dots. We tentatively identify the transition from complex E (Amin) to complex A with a possible energy-dependent step for the transposition of RNAs into the speckles. Accordingly, Ad10 and Ad11 pre-mRNAs capable of forming the prespliceosomal complex A, respectively, complex A3′ in vitro (Frendewey and Keller, 1985; Frendewey *et al.*, 1987; Christofori *et al.*, 1987) are extensively accumulated within the speckles, which have substantially increased size.

The results of comicroinjection experiments support the conclusions of experiments with RNAs microinjected individually. In addition, they further emphasize the importance of the additional 3′ sequences downstream from PPT. In this sense, the Ad8^{++} and Ad11 RNAs, containing the complete second exon and the 5′ end of the second intron, displaced the Ad8 and Ad 10 RNAs, respectively. We infer from these comicroinjection experiments that the downstream sequences stabilize the interactions with splicing factors.

The existence of sequences frequently found in the downstream exons (exonic enhancers) that stabilize the interactions in the spliceosomal complex, possibly due to the binding of SR proteins or SR-like proteins, are intensively studied at present (reviewed in Fu, 1995; Manley and Tacke, 1996; Caceres and Krainer, 1997; Wang and Manley, 1997; Blencowe, 2000). Similarly, the downstream 5′ splice site as the enhancer element has been described (Achsel and Shimura, 1996; Hwang and Cohen, 1996; Yue and Akusjärvi, 1999). The presence of the downstream enhancer in the second exon of the adenovirus RNA has also been inferred (Chew *et al.*, 1999). Furthermore, it has been shown that the downstream sequences, either in the second exon or the downstream 5′ splice site, did overcome the effects of an upstream PPT mutation in splicing (Freyer *et al.*, 1989) pointing to the presence of the splicing enhancer.

Importantly, the speckles show differences in appearance after RNA microinjection, depending on the ability of RNA to form (pre)spliceosomal complexes. The targeting of pre-mRNAs complexes to the speckles reflects the dynamics of the whole process with two interdependent features, the targeting of pre-mRNA toward the speckles and the cumulative binding (loading) of additional splicing factors giving rise to the speckle appearance. The distribution of splicing factors is changed from the initial steady state because much of the nuclear splicing machinery is recruited by the microinjected pre-mRNAs. Depending on the ability to generate certain (pre)spliceosome complexes, the appearance of the speckles is changed accordingly after microinjection. This is particularly well documented with the Ad8, Ad8^{++}, Ad10, and Ad11 RNAs, which are able to form stable (pre)spliceosomal complexes. The cumulative loading of splicing factors is also documented in the comicroinjection experiment of the Ad8 and Ad11 RNAs. The Ad11 RNA to some extent displaces the Ad8 RNA. The cumulative loading of splicing factors leading to the formation of the complete spliceosome on the Ad8 RNA largely suppresses its displacement by the Ad11 RNA (compare the difference in Figure 4, K and J).

The prominent change in the appearance of the speckles is similarly observed after the microinjection of antisense oligos that inhibit splicing (O'Keefe *et al.*, 1994). We have expanded these observations with oligos that completely inhibit, within the frame of endogenous pre-mRNAs, the formation of the prespliceosomes. The results with microinjected oligos are in agreement with exogenous pre-mRNA microinjections and indicate that the enlargement of speckles, due to the accumulation of splicing factors, reflects the accumulation of (pre)splicing complexes formed in the speckles apparently on endogenous pre-mRNA. Accordingly, U1 and U2a oligos that allow the formation of (pre-)spliceosome complex A gave rise to enlarged speckles after microinjection, whereas the U2b oligo that blocks the formation of presplicing complex completely gave rise to the speckled pattern seen in untreated cells.

How do the microinjected RNAs reflect the behavior of endogenous RNAs? A concomitant dual mechanism for the intranuclear movement of endogenous (pre)-mRNAs and splicing factors was proposed (Melčák *et al.*, 2000). Apparently, for most genes expressed at low level, splicing factors are recruited from the splicing factor reservoirs to the sites of transcription and splicing is cotranscriptional. The RNA in question is after polyadenylation ready for the export to the cytoplasm. However, if the gene is highly expressed and/or splicing slow (e.g., question of the quality and quantity of

splicing enhancers), unspliced (and polyadenylated) transcripts are released and move away from the gene toward the splicing factor reservoirs. These reservoirs may facilitate posttranscriptional splicing as suggested by Melčák and Raška (1996), Melčák *et al.* (2000), and Johnson *et al.* (2000). Generally speaking, we encounter two kinds of trafficking; the recruitment of splicing factors to transcription sites (cotranscriptional splicing) and movement of unspliced released transcripts to the splicing factor reservoirs (posttranscriptional splicing). In specific situations, one kind of trafficking may prevail over the other (for detailed discussion, see Melčák *et al.*, 2000). We are of the opinion that the behavior of microinjected pre-mRNAs is similar to those endogenous unspliced pre-mRNAs, released from the site of synthesis. There is a high demand for the splicing factors and the cumulative loading of splicing factors results in the trafficking (and accumulation) of RNAs in speckles.

The speckles are highly dynamic structures (Phair and Misteli, 2000) but the mechanisms that form and maintain this compartment in vivo are unknown. We interpret our results as pointing to a correlation between the behavior of speckles and the formation of (pre)spliceosomes, with the speckles representing the supramolecular compartment. This interpretation is in harmony with reports that although individual ~60S spliceosomes have been visualized in the in vitro systems (Reed *et al*., 1988), larger 100–300S polyspliceosomes also have been described (Wagatsuma *et al*., 1985; Wassarman and Steitz, 1993; Müller *et al*., 1998). The results of the present study show that the accumulated (pre)spliceosomal complexes give rise to the speckles. If the assembly factory corresponds to the speckles, the splicing complexes with multiple interaction sites may, through a cross-linked macromolecular network, generate the speckles, and contribute to their formation and maintenance.

ACKNOWLEDGMENTS

We thank Dr. X.-D. Fu (University of California, San Diego, CA) for the anti-SC35 antibody, and Dr. C. Will (University of Marburg, Marburg, Germany) and A. Krämer (University of Geneva, Geneva, Switzerland) for the plasmids. We thank Lucie Tomšíková for technical assistance, Professor M. Jantsch for reading the manuscript, Dr. J. Malínský for help with the preparation of Figures, and Dr. F. Raška for the English revision. This work was supported by the Wellcome Trust Grant 049949/Z/97/Z/JMW/JPS/CG, by research grants of the Grant Agency of the Czech Republic 302/99/0587 and 304/00/1481, and the grants of the Ministry of Education, Youth and Sports VS-96129 and MSM-111100003.

REFERENCES

Alberts, B., Bray, D., Lewis, J., Raff, M., Roberts, K., and Watson, D. (1994). Molecular Biology of the Cell. New York: Garland Publishing, Inc.

Achsel, T., and Shimura, Y. (1996). Factors involved in the activation of pre-mRNA splicing from downstream splicing enhancers. J. Biochem. *120*, 53–60.

Baurén, G., and Wieslander, L. (1994). Splicing of Balbiani ring 1 gene pre-mRNA occurs simultaneously with transcription. Cell *76*, 183–192.

Barabino, S.M., Blencowe, B.J., Ryder, U., Sproat, B.S., and Lamond, A.I. (1990). Targeted snRNP depletion reveals an additional role for mammalian U1 snRNP in spliceosome assembly. Cell *63*, 293–302.

Bennett, M., Michaud, S., Kingston, J., and Reed, R. (1992). Protein components specifically associated with prespliceosome and spliceosome complexes. Genes Dev. *6*, 1986–2000.

Bentley, D. (1999). Coupling RNA polymerase II transcription with pre-mRNA processing. Curr. Opin. Cell Biol. *11*, 347–351.

Beyer, A.L., and Osheim, Y.N. (1988). Splice site selection, rate of splicing, and alternative splicing on nascent transcripts. Genes Dev. *2*, 754–765.

Bindereif, A., and Green, M.R. (1987). An ordered pathway of snRNP binding during mammalian pre-mRNA splicing complex assembly. EMBO J. *6*, 2415–2424.

Blencowe, B.J. (2000). Exonic splicing enhancers: mechanism of action, diversity and role in human genetic diseases. Trends Biochem. Sci. *25*, 106–110.

Bregman, D.B., Du, L., van der Zee, S., and Warren, S.L. (1995). Transcription-dependent redistribution of the large subunit of RNA polymerase II to discrete nuclear domains. J. Cell Biol. *129*, 287–298.

Caceres, J.F., and Krainer, A.R. (1997). Mammalian pre-mRNA splicing factors. In: Eukaryotic mRNA Processing, ed. A.R. Krainer, Oxford: IRL Press, 174–212.

Chew, L.S., Liu, H.X., Mayeda, A., and Krainer, R.A. (1999). Evidence for the function of an exonic splicing enhancer after the first catalytic step of pre-mRNA splicing. Proc. Natl. Acad. Sci. USA *96*, 10655–10660.

Christofori, G., Frendewey, D., and Keller, W. (1987). Two spliceosomes can form simultaneously and independently on synthetic double-intron messenger RNA precursors. EMBO J. *6*, 1747–1755.

Corden, J.L., and Patturajan, M. (1997). A CTD function linking transcription to splicing. Trends Biochem. Sci. *22*, 413–416.

Custodio, N., Carmo-Fonseca, M., Geraghty, F., Pereira, H., Grosveld, F., and Antoniou, M. (1999). Inefficient processing impairs release of RNA from the site of transcription. EMBO J. *18*, 2855–2866.

Dirks, R.W., de Pauw, E.S.D., and Raap, A.K. (1997). Splicing factors associate with nuclear H.C.M.V-IE. transcripts after transcriptional activation of the gene, but dissociate upon transcription inhibition: evidence for a dynamic organization of splicing factors. J. Cell Sci. *110*, 505–513.

Fakan, S. (1994). Perichromatin fibrils are in situ forms of nascent transcripts. Trends Cell Biol. *4*, 86–90.

Fakan, S., and Puvion, E. (1980). The ultrastructural visualization of nucleolar and extranucleolar RNA synthesis and distribution. Int. Rev. Cytol. *65,* 255–299.

Frendewey, D., and Keller, W. (1985). Stepwise assembly of a pre-mRNA splicing complex requires U-snRNPs and specific intron sequences. Cell *42*, 355–367.

Frendewey, D., Krämer, A., and Keller, W. (1987). Different small nuclear ribonucleoprotein particles are involved in different steps of splicing complex formation. Cold Spring Harbor Symp. Quant. Biol. *52*, 287–298.

Freyer, G.A., O'Brien, J.P., and Hurwitz, J. (1989). Alterations in the polypyrimidine sequence affect the in vitro splicing reactions catalyzed by HeLa cell-free preparations. J. Cell Chem. *264*, 14631–14637.

Fu, X.D. (1995). The superfamily of arginine/serine-rich splicing factors. RNA *1*, 663–680.

Fu, X.D., and Maniatis, T. (1990). Factor required for mammalian spliceosome assembly is localized to discrete regions in the nucleus. Nature *343*, 437–441.

Graessmann, M., and Graessmann, A. (1982). Simian virus 40 cRNA is processed into functional mRNA in microinjected monkey cells. EMBO J. *1*, 1081–1088.

Hamm, J., Dathan, N.A., and Mattaj, I.W. (1989). Functional analysis of mutant *Xenopus* U2 snRNAs. Cell *59*, 159–169.

Hamm, J., and Mattaj, I.W. (1990). Monomethylated cap structures facilitate RNA export from the nucleus. Cell *63*, 109–118.

Hoffman, B.E., and Grabowski, P.J. (1992). U1 snRNP targets an essential splicing factor, U2AF65, to the 3′ splice site by a network of interactions spanning the exon. Genes Dev. *6*, 2554–2568.

Huang, S., and Spector, D.L. (1996). Intron-dependent recruitment of pre-mRNA splicing factors to sites of transcription. J. Cell Biol. *133*, 719–732.

Hwang, D.Y., and Cohen, J.B. (1996). Base pairing at the 5′ splice site with U1 small nuclear RNA promotes splicing of the upstream intron but may be dispensable for splicing of the downstream intron. Mol. Cell. Biol. *16*, 3012–3022.

Ishov, A.M., Stenberg, R.M., and Maul, G.G. (1997). Human cytomegalovirus immediate early interaction with host nuclear structures: definition of an immediate transcript environment. J. Cell Biol. *138*, 5–16.

Jacobson, M.R., Cao, L.G., Wang, Y.L., and Pederson, T. (1995). Dynamic localization of RNase MRP RNA in the nucleolus observed by fluorescent RNA cytochemistry in living cells. J. Cell Biol. *131*, 1649–1658.

Jacobson, M.R., Cao, L.G., Taneja, K., Singer, R.H., Wang, Y.L., and Pederson, T. (1997). Nuclear domains of the RNA subunit of RNase P. J. Cell Sci. *110*, 829–837.

Jacobson, M.R., and Pederson, T. (1998a). Localization of signal recognition particle RNA in the nucleolus of mammalian cells. Proc. Natl. Acad. Sci. USA *95*, 7981–7986.

Jacobson, M.R., and Pederson, T. (1998b). A 7-methylguanosine cap commits U3 and U8 small nuclear RNAs to the nucleolar localization pathway. Nucleic Acids Res. *26*, 756–760.

Jamison, S.F., Crow, A., and Garcia-Blanco, M.A. (1992). The spliceosome assembly pathway in mammalian extracts. Mol. Cell. Biol. *12*, 4279–4287.

Johnson, C., Primorac, D., McKinstry, M., McNeil, J., Rowe, D., and Lawrence, J.B. (2000). Tracking COL1A1 RNA in Osteogenesis Imperfecta: splice-defective transcripts initiate transport from the gene but are retained within the SC35 domain. J. Cell Biol. *150*, 417–431.

Koberna, K., Staněk, D., Malínský, J., Eltsov, M., Plis, A., Ctrnáctá, V., Cermanová, Š., and Raška, I. (1999). Nuclear organization studied with the help of a hypotonic shift: its use permits hydrophilic molecules to enter into living cells. Chromosoma *108*, 325–335.

Konarska, M.M., and Sharp, P.A. (1986). Electrophoretic separation of complexes involved in the splicing of precursors to mRNAs. Cell *46*, 845–855.

Konarska, M.M., and Sharp, P.A. (1987). Interactions between small nuclear ribonucleoprotein particles in formation of spliceosomes. Cell *49*, 763–774.

Krause, S., Fakan, S., Weis, K., and Wahle, E. (1994). Immunodetection of poly(A) binding protein II in the cell nucleus. Exp. Cell Res. *214*, 75–82.

Krämer, A. (1996). The structure and function of proteins involved in mammalian pre-mRNA splicing. Annu. Rev. Biochem. *65*, 367–409.

Lamm, G.M., and Lamond, A.I. (1993). Non-snRNP protein splicing factors. Biochim. Biophys. Acta *1173*, 247–265.

Lamond, A.I. (1999). RNA splicing. Running rings around RNA. Nature *397*, 655–656.

Lamond, A.I., Sproat, B., Ryder, U., and Hamm, J. (1989). Probing the structure and function of U2 snRNP with antisense oligonucleotides made of 2′-OMe RNA. Cell 58, 383–390.

Larsson, S.H., Charlieu, J.P., Miyagawa, K., Engelkamp, D., Rassoulzadegan, M., Ross, A., Cuzin, F., van Heyningen, V., and Hastie, N.D. (1995). Subnuclear localization of WT1 in splicing or transcription factor domains is regulated by alternative splicing. Cell *81*, 391–401.

Legrain, P., Seraphin, B., and Rosbash, M. (1988). Early commitment of yeast pre-mRNA to the spliceosome pathway. Mol. Cell. Biol. *8*, 3755–3760.

Manley, J.L., and Tacke, R. (1996). SR proteins and splicing control. Genes Dev. *10*, 1569–1579.

Mattaj, I.W. (1994). RNA processing. Splicing in space. Nature *372*, 727–728.

McCracken, S., Fong, N., Yankulov, K., Ballantyne, S., Pan, G., Greenblatt, J., Patterson, S.D., Wickens, M., and Bentley, D.L. (1997). The C-terminal domain of RNA polymerase II couples mRNA processing to transcription. Nature *385*, 357–361.

Melčák, I., and Raška, I. (1996). Structural organization of the pre-mRNA splicing commitment. A hypothesis. J. Struct. Biol. 117, 189–194.

Melčák, I., Cermanová, Š., Jirsová, K., Koberna, K., Malínský, J., and Raška, I. (2000). Nuclear pre-mRNA compartmentalization: trafficking of released transcripts to splicing factor reservoirs. Mol. Biol. Cell *11*, 497–510.

Michaud, S., and Reed, R. (1991). An ATP-independent complex commits pre-mRNA to the mammalian spliceosome assembly pathway. Genes Dev. *5*, 2534–2546.

Michaud, S., and Reed, R. (1993). A functional association between the 5′ and 3′ splice site is established in the earliest prespliceosome complex (E) in mammals. Genes Dev. *7*, 1008–1020.

Minvielle-Sebastia, L., and Keller, W. (1999). mRNA polyadenylation and its coupling to other RNA processing reactions and to transcription. Curr. Opin. Cell Biol. *11*, 352–357.

Misteli, T. (2000). Cell biology of transcription and pre-mRNA splicing: nuclear architecture meets nuclear function. J. Cell Sci. *113*, 1841–1849.

Misteli, T., Cáceres, J.F., and Spector, D.L. (1997). The dynamics of a pre-mRNA splicing factor in living cells. Nature *387*, 523–527.

Misteli, T., and Spector., D.L. (1998). RNA polymerase II targets pre-mRNA splicing factors to transcription sites in vivo. Mol. Cell *3*, 697–705.

Moore, M.J., Query, C.C., and Sharp, P.A. (1993). Splicing of precursors to messenger RNAs by the spliceome. In: The RNA World, ed. R.F. Gesteland and J.F. Atkins, Cold Spring Harbor, NY: CSHL Press, 303–357.

Müller, S., Wolpensinger, B., Angenitzki, M., Engel, A., Sperling, J., and Sperling, R. (1998). A supraspliceosome model for large nuclear ribonucleoprotein particles based on mass determinations by scanning transmission electron microscopy. J. Mol. Biol. *283*, 383–394.

Neugebauer, K.M., and Roth, M.B. (1997). Distribution of pre-mRNA splicing factors at sites of RNA polymerase II transcription. Genes Dev. *11*, 1148–1159.

Newman, A.J. (1994). Small nuclear RNAs and pre-mRNA splicing. Curr. Opin. Cell Biol. *6*, 360–367.

Newman, A.J. (1998). RNA splicing. Curr. Biol. *8*, 17–31.

O'Keefe, R.T., Mayeda, A., Sadowski, C.L., Krainer, A.R., and Spector, D.L. (1994). Disruption of pre-mRNA splicing in vivo results in reorganization of splicing factors. J. Cell Biol. *124*, 249–260.

Pan, Z.Q., and Prives, C. (1988). Assembly of functional U1 and U2 human-amphibian hybrid snRNPs in *Xenopus laevis* oocytes. Science *241*, 1328–1331.

Pederson, T. (1998). The plurifunctional nucleolus. Nucleic Acids Res. *26*, 3871–3876.

Pederson, T. (1999). Movement and localization of RNA in the cell nucleus. FASEB J. *13(suppl 2)*, S238–S242.

Perraud, M., Gioud, M., and Monier, J.C. (1979). Intranuclear structures of monkey kidney cells recognized by immunofluorescence and immuno-electron microscopy using antiribonucleoprotein antibodies. Ann. Immunol. *130C*, 635–647.

Phair, R.D., and Misteli, T. (2000). High mobility of proteins in the mammalian cell nucleus. Nature *404*, 604–609.

Politz, J.C., Tuft, R.A., Pederson, T., and Singer, R.H. (1999). Movement of nuclear poly(A)RNA throughout the interchromatin space in living cells. Curr. Biol. *9*, 285–291.

Puvion, E., Viron, A., Assens, C., Leduc, E.H., and Jeanteur, P. (1984). Immunocytochemical identification of nuclear structures containing snRNPs in isolated rat liver cells. J. Ultrastruct. Res. *87*, 180–189.

Query, C.C., McCaw, P.S., and Sharp, P.A. (1997). A minimal spliceosomal complex A recognizes the branch site and polypyrimidine tract. Mol. Cell. Biol. *17*, 2944–2953.

Raška, I. (1995). Nuclear ultrastructures associated with the RNA synthesis and processing. J. Cell Biochem. *59*, 11–26.

Reed, R., Griffith, J., and Maniatis, T. (1988). Purification and visualization of native spliceosomes. Cell *53*, 949–961.

Rossi, F., Forne, T., Antoine, E., Tazi, J., Brunel, C., and Cathala, G. (1996). Involvement of U1 small nuclear ribonucleoproteins (snRNP) in 5′ splice site-U1 snRNP interaction. J. Biol. Chem. *271*, 23985–23991.

Seiwert, S.D., and Steitz, J.A. (1993). Uncoupling two functions of the U1 small nuclear ribonucleoprotein particle during in vitro splicing. Mol. Cell. Biol. *13*, 3134–3145.

Seraphin, B., and Rosbash, M. (1989). Identification of functional U1 snRNA-pre-mRNA complexes committed to spliceosome assembly and splicing. Cell *59*, 349–358.

Sharp, P.A. (1994). Split genes and RNA splicing. Cell *77*, 805–815.

Sinclair, G.D., and Brasch, K. (1978). The reversible action of α-amanitin on nuclear structure and molecular composition. Exp. Cell Res. *111*, 1–14.

Smith, K.P., Moen, P.T., Wydner, K.L., Coleman, J.R., and Lawrence, J.B. (1999). Processing of endogenous pre-mRNAs in association with SC-35 domains is gene specific. J. Cell Biol. *144*, 617–629.

Snaar, S.P., Vincent, M., and Dirks, R.W. (1999). RNA polymerase II localizes at sites of human cytomegalovirus immediate-early RNA synthesis and processing. J. Histochem. Cytochem. *47*, 245–254.

Spector, D.L. (1990). Higher order nuclear organization: three-dimensional distribution of small nuclear ribonucleoprotein particles. Proc. Natl. Acad. Sci. USA *87*, 147–151.

Spector, D.L., Fu, X.D., and Maniatis, T. (1991). Associations between distinct pre-mRNA splicing components and the cell nucleus. EMBO J. *10*, 3467–3481.

Spector, D.L., Schrier, W.H., and Busch, H. (1983). Immunoelectron microscopic localization of snRNPs. Biol. Cell *49*, 1–10.

Staknis, D., and Reed, R. (1994). SR proteins promote the first specific recognition of pre-mRNA and are present together with the U1 small nuclear ribonucleoprotein particle in a general splicing enhancer complex. Mol. Cell. Biol. *14*, 7670–7682.

Steitz, J.A., Black, D.A., Gerke, V., Parker, K.A., Krämer, A., Frendewey, D., and Keller, W. (1988). Functions of the abundant U-snRNPs. In: Structure and Function of Major and Minor Small Nuclear Ribonucleoprotein Particles, ed. M.L. Birnstiel, Berlin: Springer Verlag, 71–99.

Vankan, P., McGuigan, C., and Mattaj, I.W. (1992). Roles of U4 and U6 snRNAs in the assembly of splicing complexes. EMBO J. *11*, 335–343.

Wagatsuma, M., Obinata, M., Moroi, Y., Hanaoka, F., and Yamada, M. (1985). Detection of beta-globin mRNA precursor in heterogeneous nuclear ribonucleoprotein associated with U1-RNP by using anti-RNP antibody. J. Biochem. *97*, 1727–1735.

Wang, J., Cao, L.G., Wang, Y.L., and Pederson, T. (1991). Localization of pre-messenger RNA at discrete nuclear sites. Proc. Natl. Acad. Sci. USA *88*, 7391–7395.

Wang, J., and Manley, J.L. (1997). Regulation of pre-mRNA splicing in metazoa. Curr. Opin. Genet. Dev. *7*, 205–211.

Wansink, D.G., Nelissen, R.L., and de Jong, L. (1994). In vitro splicing of pre-mRNA containing bromouridine. Mol. Biol. Rep. *19*, 109–113.

Wassarman, D.A., and Steitz, J.A. (1993). A base–pairing interaction between U2 and U6 small nuclear RNAs occurs in >150S complexes in HeLa cell extracts: implications for the spliceosome assembly pathway. Proc. Natl. Acad. Sci. USA *90*, 7139–7143.

Wuarin, J., and Schibler, U. (1994). Physical isolation of nascent RNA chains transcribed by RNA polymerase II: evidence for cotranscriptional splicing. Mol. Cell. Biol. *14*, 7219–7225.

Xing, Y., Johnson, C.V., Dobner, P., and Lawrence, J.B. (1993). Higher level organization of individual gene transcription and RNA splicing: integration of nuclear structure and function. Science *259*, 1326–1330.

Xing, Y., Johnson, C.V., Moen, P.T., Jr., McNeil, J.A., and Lawrence, J.B. (1995). Nonrandom gene organization: structural arrangements of specific pre-mRNA transcription and splicing with SC-35 domains. J. Cell Biol. *131*, 1635–1647.

Yue, B.G., and Akusjärvi, G. (1999). A downstream splicing enhancer is essential for in vitro pre-mRNA splicing. FEBS Lett. *451*, 10–14.

Zachar, Z., Kramer, J., Mims, I.P., and Bingham, P.M. (1993). Evidence for channeled diffusion of pre-mRNAs during nuclear RNA transport in metazoans. J. Cell Biol. *121*, 729–742.

Zhang, G., Taneja, K.L., Singer, R.H., and Green, M.R. (1994). Localization of pre-mRNA splicing in mammalian nuclei. Nature *372*, 809–812.

Zillmann, M., Zapp, M.L., and Berget, S.M. (1988). Gel electrophoretic isolation of splicing complexes containing U1 snRNPs. Mol. Cell. Biol. *8*, 814–821.